Molecular Engineering of Potent Sensitizers for Very Efficient Light Harvesting in Thin-Film Solid-State Dye-Sensitized Solar Cells

Molecular engineering of potent sensitizers for very efficient light harvesting in thin film solid state dye sensitized solar cells

Xiaoyu Zhang[a,b,‡], Yaoyao Xu[a,‡], Fabrizio Giordano[b,*], Marcel R. Schreier[b], Norman Pellet[b], Yue Hu[c], Chenyi Yi[b], Neil Robertson[c], Jianli Hua[a,*], Shaik M. Zakeeruddin[b,*], He Tian[a], and Michael Grätzel[b,*]

[a] Key Laboratory for Advanced Materials and Institute of Fine Chemicals, School of Chemistry and Molecular Engineering, East China University of Science and Technology, 130 Meilong Road, Shanghai 200237, China

[b] Laboratoire de Photoniques et Interfaces, Institut des Sciences et Ingénierie Chimiques, École Polytechnique Fédérale de Lausanne, Station 6, 1015 Lausanne, Switzerland

[c] School of Chemistry, University of Edinburgh, King's Buildings, Edinburgh, EH9 3FJ, UK.

Supporting Information Placeholder

ABSTRACT: Dye-sensitized solar cells (DSSCs) have shown significant potential for indoor and building integrated photovoltaic applications. Herein we present three new D-A-π-A organic sensitizers, **XY1**, **XY2** and **XY3**, exhibiting high molar extinction coefficients and a broad absorption range. Molecular modifications of these dyes, featuring a benzothiadiazole (BTZ) auxillary acceptor, were achieved by introducing a thiophene heterocycle, as well as by shifting the position of BTZ on the conjugated bridge. The ensuing high molar absorption coefficients enable highly efficient thin-film solid-state dye-sensitized solar cells with only 1.3 μm mesoporous TiO_2 layer. **XY2** with a molar extinction coefficient of 6.66×10^4 M^{-1} cm^{-1} at 578 nm led to the best photovoltaic performance of 7.51%.

After 25 years of thorough study and development, dye-sensitized solar cells (DSSCs) are nowadays moving towards industrial production, aided by their simple and low-cost fabrication process, large range of colors, transparency and high photovoltaic conversion efficiency (PCE), particularly under low illumination conditions.[1,2] Solid-state DSSCs (ssDSSCs) employing hole-transporting materials (HTMs) instead of redox shuttles in solution, have attracted significant interest as a practical solution for the problems posed by traditional liquid electrolytes.[3-5] In 1998, Spiro-OMeTAD (2,2',7,7'-tetrakis(N,N-di-*p*-methoxyphenylamine)-9,9'-spirobifluorene) was reported as the first HTM for ssDSSCs. This material has since been widely used, not only in ssDSSCs but also in perovskite solar cells.[4,6-8] A challenge for ssDSSC applications, however, remains the fact that spiro-OMeTAD only insufficiently infiltrates into thick mesoporous TiO_2 films. These films are therefore limited to a thickness of about 2 – 5 um. [9,10] Therefore, dyes with high extinction coefficients and broad absorption range are of great importance in order to achieve high solar-to-electricity conversion efficiencies on thin TiO_2 layers in ssDSSCs. Highly performing ssDSSCs, exibiting

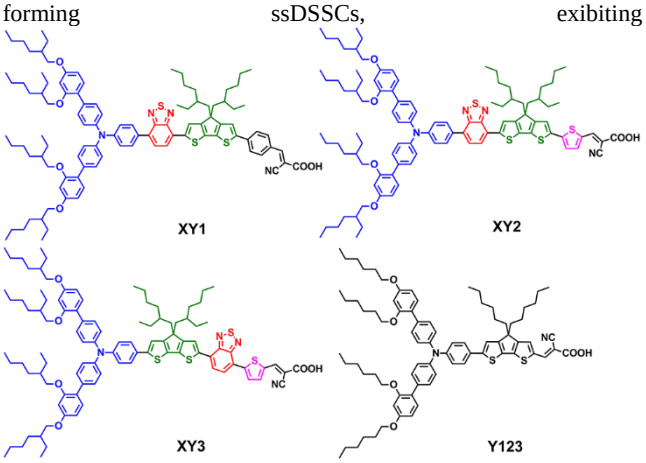

Figure 1. Molecular structures of **XY1**, **XY2**, **XY3** and **Y123**.

thin TiO_2 layers and strongly absorbing dyes do also not require scattering layers for optimal light harvesting. It is for this reason that they are very promising candidates for future application in building-integrated photovoltaic windows and other areas, where aesthetics play an important role. Organic sensitizers are ideal candidates for thin film cells due to their significantly higher molar extinction coefficients and lower cost than ruthenium-based sensitizers. Furthermore, their structural flexibility allows accessing a larger parameter space for fine tuning of dye properties.[11-13] This is particularly important in the case of dye regeneration and charge recombination processes at the TiO_2/dye/HTM interface, where molecular-level modifications of organic sensitizers are employed as an effective approach to impede undesirable charge recombination processes.[13-15] This is exemplified in the case of **Y123** (**Figure 1**) and **LEG4,** featuring bulky donors and cyclopentadithiophene

(CPDT)-based π-bridges, protected by alkoxy and alkyl chains, respectively. These bulky side chains shield the dye from the oxidized HTM and thereby inhibit recombination at the interface of TiO_2/dye/HTM, leading to highly efficient ssDSSCs with spiro-OMeTAD.[16-18] For example, Burschka et. al. achieved a PCE of 7.2% from **Y123**-sensitized ssDSSCs using tris(2-(1H-pyrazol-1-yl)pyridine)cobalt(III) (**FK102**) as p-type HTM dopant (film thickness: 2.5 µm). [16] Similarly, **LEG4**-sensitized ssDSSCs obtained a PCE of 7.7% with 1,1,2,2-tetracholoroethane-doped spiro-OMeTAD (film thickness: ~ 2.5 µm)[18] and 8.2% with copper phenanthroline as hole conductor (film : ~ 6 µm transparent + 3 µm scattering layer)[19].

Previous work on DSSCs from our own, as well as Zhu's group demonstrated, that organic sensitizers with D-A-π-A structures outperform their D-π-A analogues because the introduction of an auxiliary acceptor between the donor and π-bridge facilitates fine-tuning of the molecular energy levels. This leads to increased absorption and to an extension of the spectral response towards the red.[13,20,21] From these works, benzothiadiazole (BTZ) emerged as a promising acceptor functionality.[20,22] Following these results, we here investigated three novel BTZ-based D-A-π-A sensitizers, **XY1**, **XY2** and **XY3** (**Figure 1**). **XY1** showed a high molar extinction coefficient, which could further be increased in **XY2** by introducing a heterocyclic thiophene unit onto the conjugated chain, also leading to an extension of the absorption towards the red. This effect was further enhanced upon exchanging the position of BTZ and CPDT, **XY3**, yielding a dye that absorbed up to the near infrared region. The high molar extinction coefficients obtained from **XY1** and **XY2** enabled the fabrication of devices using very thin mesoporous TiO_2 layers (~ 1.3 µm), without compromising on device performance.

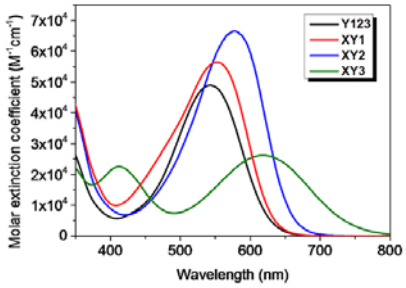

Figure 2. Absorption spectra of **Y123** (black) and **XY1**(red), **XY2** (blue), and **XY3** (green) in CH_2Cl_2.

Table 1. Optical and electrochemical properties of **XY1, XY2, XY3** and **Y123.**

Dye	λ_{max}[a]/nm ($\varepsilon\times10^4$ $M^{-1}cm^{-1}$)	HOMO[b]/V (vs. NHE)	$E_{0\text{-}0}$[c] /eV	LUMO[d]/V (vs. NHE)
Y123	543 (4.90)	0.92	2.01	-1.09
XY1	552 (5.65)	0.99	1.97	-0.98
XY2	578 (6.66)	0.91	1.92	-1.01
XY3	618 (2.62)	0.75	1.80	-1.05

[a] Absorption maximum in CH_2Cl_2 solution. [b] measured in CH_2Cl_2 with 0.1 M tetra-n-butylammonium hexafluorophosphate ($TBAPF_6$) as electrolyte (working electrode: Pt; counter electrode: Pt wire; reference electrode: SCE; calibrated with ferrocene/ ferrocenium (Fc/Fc^+) as an external reference). [c] $E_{0\text{-}0}$ was estimated from the absorption onset wavelength from UV-Vis absorption spectra of the dyes. [d] LUMO was estimated by subtracting $E_{0\text{-}0}$ from E_{HOMO}.

The absorption spectra of **XY1**, **XY2**, **XY3** as well as the reference dye **Y123** in CH_2Cl_2 are shown in **Figure 2** whilst the parameters of their optical and electrochemical properties are displayed in **Table 1**. The main absorption band can be assigned to the intramolecular charge transfer (ICT) between the bulky donor and the cyanoacetic acid acceptor moiety.[13,23] From **Figure 2**, we can clearly see that **XY1** and **XY2** not only show bathochromic shifts of the low energy absorption band but also an increase in molar extinction coefficients compared to **Y123**. Among the investigated structures, **XY2** emerges as the most suitable sensitizer for ssDSSC due to its high molar extinction coefficient of 6.66×10^4 M^{-1} cm^{-1} at its maximum absorption wavelength of 578 nm. Interestingly, by switching the position of BTZ and CPDT (**XY3**), the absorption band was largely extended to the near infrared region, red-shifting the low energy absorption peak by 40 nm compared to **XY2**. However, the molar extinction coefficient of **XY3** drops to 2.62×10^4 $M^{-1}cm^{-1}$. At the same time, the HOMO energy level of **XY3** was upshifted to 0.75 V vs. NHE, whilst **XY2** has its HOMO energy level at 0.91 V vs. NHE, similar to that of **Y123** and **XY1**. Density functional theory (DFT) calculations revealed better overlap of the HOMO and LUMO orbitals in **XY2**, **XY1** and **Y123** than **XY3** (**Figure S1**), which provides a likely explanation for the higher molar extinction coefficients of **XY2**, **XY1** and **Y123** compared to **XY3**.[24] From these data, it could also be noticed that CPDT contributes to electron donation in **XY3**, **Figure S1**, thereby shifting the HOMO energy level upwards.

In order to test the performance of these dyes in an ssDSSC application, devices were prepared using spin coated thin transparent mesoporous TiO_2 layers. The resulting **XY2**-sensitized ssDSSC devices showed a reddish-purple color and substantial transparency of the light absorbing layer as shown in **Figure 3 (a)**. The cross-sectional SEM micrograph of the same device, **Figure 3 (b)**, shows that spiro-OMeTAD penetrates the entire mesoporous structure, while exhibiting a 100 nm capping layer on the surface, isolating the TiO_2 film from the Au counter electrode.

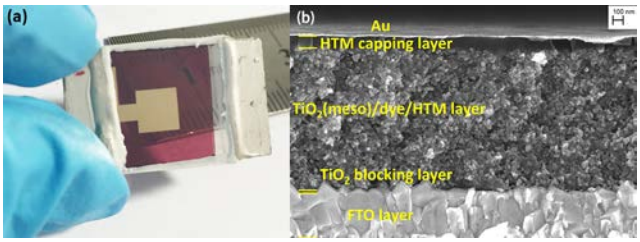

Figure 3. Photograph (a) and cross section SEM image (b) of ssDSSC device based on **XY2** with a ~1.3 µm-thick transparent mesoporous TiO_2 layer.

The photovoltaic performance of ssDSSCs based on **Y123**, **XY1**, **XY2** and **XY3** under different light intensities are tabulated in **Table 2** and their corresponding current densitiy-voltage (*J-V)* curves, dark current plots and incident photon-to-electron conversion efficiency (IPCE) spectra are displayed in **Figure 4**. Solid-state DSSC with 1.3 µm TiO_2 films showed good reproducibility (**Figure S3**). **XY1** and **XY2** perform significantly better than **Y123** in ssDSSC devices due to their high molar extinction coefficients. The short circuit current densities (J_{sc}) of ssDSSC devices with **XY1** and **XY2** reached over 10 $mAcm^{-2}$, which exceeds the 8.45 $mAcm^{-2}$ observed from **Y123**. For devices based on the green dye **XY3**, a J_{sc} of 11.06 $mAcm^{-2}$ was obtained but with a considerably lower V_{oc} value, losing over 100 mV compared to the other dyes. A V_{oc} of 0.798 V, 0.929 V, 0.942 V and 0.904 V was obtained with **XY3**, **XY2**, **XY1** and **Y123**, respectively. Devices based on **XY2** and **XY1** led to good PCEs of 6.89% and 6.69%, respectively under 95% Sun illumination, considerably higher than devices based on the reference dye **Y123 (**5.77%). A PCE of 5.50% was obtained for **XY3**, which is remarkable since its HOMO energy level is very

close to that of Spiro-OMeTAD, suggesting that the dye regeneration takes place despite the small driving force between the HOMO levels of dye and HTM. The lower V_{oc} potentially indicates increased electron recombination at the TiO_2/dye/HTM interface. This effect will be further investigated below. PCEs under 50% and 10% light intensity were also measured, illustrating excellent potential for Building Integrated Photovoltaic (BIPV) applications. Beyond 500 nm, devices based on **XY1** and **XY2** showed much higher IPCE than **Y123**. The peak IPCE was found to be 71% at 560 nm for **XY1** and 70% at 580 nm for **XY2**, in contrast to 63% at 480 nm for **Y123**-based devices. In analogy to its absorption spectrum, devices based on **XY3** showed two absorption peaks with IPCEs of 60% at 590 nm and 50% at 430 nm, respectively. The photovoltaic performance of ssDSSCs based on these dyes was assessed as a function of film thickness, ranging from 0.25 μm to 2.0 μm (see Supporting Information, section 8 and 9). Amazingly, with a TiO_2 film as thin as ~250 nm, ssDSSCs based on **XY2** and **XY1** reached PCEs of 4.34% and 4.01%, respectively.

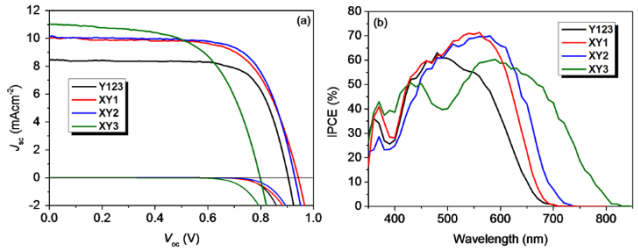

Figure 4. (a) *I-V* curves and dark currents of ssDSSCs with ~1.3 μm-thick TiO_2 layers based on **Y123** (black) and **XY1** (red), **XY2**(blue), and **XY3**(green) and (b) their corresponding IPCE plots under illumination of 10% Sun.

Table 2. Performance parameters of ssDSSCs based on **XY1, XY2, XY3** and **Y123** under different light intensities (I_0).

Dye	I_0/Sun	V_{oc}/V	J_{sc}/mA cm^{-2}	FF	PCE/%
Y123	96.6%	0.904	8.45	0.729	5.77
	49.9%	0.875	4.40	0.760	5.87
	9.3%	0.804	0.80	0.784	5.44
XY1	95.0%	0.942	10.02	0.674	6.69
	49.4%	0.907	5.31	0.717	6.98
	9.2%	0.815	0.95	0.767	6.46
XY2	95.5%	0.929	10.14	0.698	6.89
	50.1%	0.900	5.31	0.736	7.02
	9.2%	0.823	1.00	0.774	6.89
XY3	95.6%	0.798	11.06	0.596	5.50
	49.3%	0.774	5.67	0.656	5.85
	9.3%	0.703	0.98	0.683	5.06

The **XY2**-sensitized champion device achieved a PCE of 7.51%. This device also showed excellent PCEs under low light intensities (**Table 3** and **Figure 5**). Under 50% Sun illumination, a high PCE of 7.64% was reached, which still amounted to 7.00% below 10% Sun. Current dynamics measurements of photocurrent vs. light intensity are shown in **Figure 5(b)**. These measurements demonstrate a significant linearity between photocurrent and light intensity, suggesting that the photogenerated charges are efficiently evacuated in the investigated device.

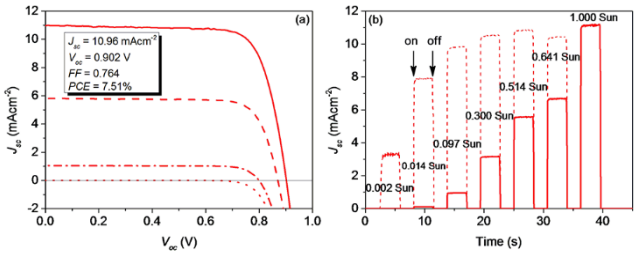

Figure 5. (a) *I-V* curves of champion **XY2**-sensitized ssDSSC device under different light intensities (solid: 1 Sun; dash: 0.5 Sun; dash dot: 0.1 Sun; dot: dark) and (b) the current dynamics (solid: measured data; dot, integrated results under 1 Sun).

Table 3. Performance parameters of champion ssDSSC based on **XY2** under different light intensities (I_0).

I_0/Sun	V_{oc}/V	J_{sc}/mAcm^{-2}	FF	PCE/%
100.5%	0.902	10.96	0.764	7.51
51.7%	0.870	5.80	0.785	7.64
9.6%	0.799	1.05	0.803	7.00

In order to better understand the relationship between the molecular structure of the dye and the resulting device performance, we performed charge extraction and transient optoelectronic analyses. Two devices were measured for each dye. The voltage vs. charge plot (**Figure 6a**) showed a weak upward shift of the electron quasi fermi level in TiO_2 for **XY1** and **XY2** when compared to **Y123**. No shift was found for **XY3**. The higher open circuit voltage of the devices employing **XY**1 and **XY2** compared to **Y123** is in good agreement with these charge extraction measurement. The higher voltage is likely related to the more efficient photo-conversion of the dyes with higher molar extinction coefficients. Moreover, the energetics of the TiO_2 conduction band are affected by the dipole generated by the surface adsorbed dye and a downward shift of the conduction band is expected to be directly proportional to the number of dye molecules covering the surface.[25] An increase in the molecular size will result in a decreased dye loading on the TiO_2 surface,[26] which in turn would expose more bare TiO_2 surface to the Spiro-OMeTAD thus increasing the recombination rate. This reasoning is in agreement with the data on electron lifetime shown in in **Figure 6b**. For **XY1** and **XY2** the electron lifetime is 3 to 2 times lower compared to **Y123**, depending on the illumination condition.

The lower open circuit voltage of the devices employing **XY3** is directly related to the electron lifetime. From **Figure 6b** it becomes clear that the recombination is ten times faster for **XY3** compared to **Y123**. The higher recombination rate is thus responsible for the 100 mV difference in V_{oc} between these dyes. We suggest that the presence of an auxiliary acceptor close to the TiO_2 surface could play a role in accelerating the recombination rate in concomitance with its lower driving force for regeneration.[27] Interestingly, we observed slightly longer electron transport time constants for **XY1** and **XY2** compared to **Y123** and **XY3**, as shown in **Figure 6c**.

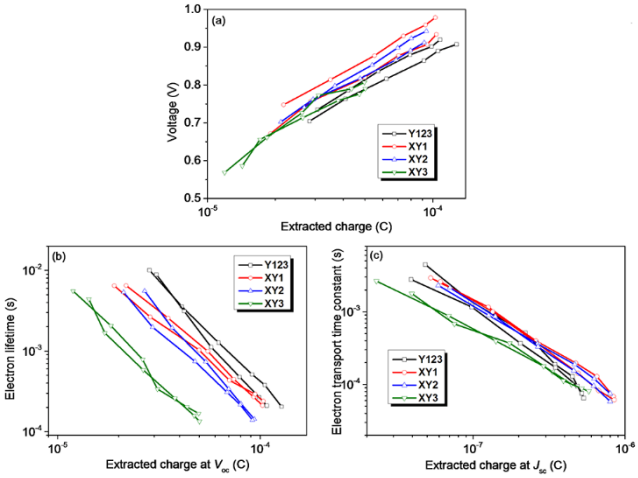

Figure 6. Voltage (a) and electron lifetime (b) vs. extracted charge at V_{oc} and electron transport time constant (c) vs. extracted charge at J_{sc} in ssDSSCs based on **Y123** (black) and **XY1**(red), **XY2**(blue), and **XY3**(green).

In conclusion, through rational molecular structure modifications, we designed and investigated three novel organic sensitizers **XY1**, **XY2** and **XY3**, among which **XY1** and **XY2** exhibit very high molar extinction coefficients and **XY3** shows a board absorption range reaching the near infrared region. By these modifications, we were able to achieve the best efficiency reported to date for D-A-π-A sensitizers in a ssDSSC application. With a TiO_2 film thickness of ~1.3 μm, ssDSSCs based on **XY1** and **XY2** reached impressively high PCEs of 6.69% and 6.89%, much higher than for **Y123**. The champion device based on **XY2** achieved a PCE of 7.51%. Despite the small offset between the HOMO energy levels of **XY3** and spiro-OMeTAD, PCE of 5.50% was achieved in the ssDSSC using this dye. However, **XY3** led to more charge recombination, which was attributed to the short electron lifetime and low driving force for dye regeneration, thus resulting in a low device V_{oc}.

ASSOCIATED CONTENT

Supporting Information

Details for regents, materials, instruments and characterization. Synthetic routes, procedures and characterization data of all the new compounds. Methodology and results of density functional theory calculations. Details for fabrication of ssDSSCs, photovoltaic measurement and phototransient measurement. Results of reproducibility test and photovoltaic performance of ssDSSCs with different film thickness.

AUTHOR INFORMATION

Corresponding Author

fabrizio.giordano@epfl.ch
jlhua@ecust.edu.cn
shaik.zakeer@epfl.ch
michael.graetzel@epfl.ch

Author Contributions

‡These authors contributed equally.

Notes

The authors declare no competing financial interests.

ACKNOWLEDGMENT

This work was supported by NSFC for Creative Research Groups (21421004), NSFC/China (21372082, 21572062 and 91233207) and the Programme of Introducing Talents of Discipline to Universities (B16017). Zhang thanks the China Scholarship Council (CSC) for the financial support of a visiting program at EPFL. MS thanks Siemens AG for funding. MG acknowledges financial support from Swiss National Science Foundation and CTI 17622.1 PFNM-NM, glass2energy sa (g2e), Villaz-St-Pierre, Switzerland.

REFERENCES

(1) O'Regan, B.; Grätzel, M. *Nature* **1991**, *353*, 737.
(2) Hagfeldt, A.; Boschloo, G.; Sun, L. C.; Kloo, L.; Pettersson, H. *Chem. Rev.* **2010**, *110*, 6595.
(3) Grätzel, M. *MRS Bulletin* **2005**, *30*, 23
(4) Yum, J.-H.; Chen, P.; Grätzel, M.; Nazeeruddin, M. K. *ChemSusChem* **2008**, *1*, 699
(5) Vlachopoulos, N.; Zhang, J.; Hagfeldt, A. *Chimia* **2015**, *69*, 41
(6) Bach, U.; Lupo, D.; Comte, P.; Moser, J. E.; Weissörtel, F.; Salbeck, J.; Spreitzer, H.; Grätzel, M. *Nature* **1998**, *395*,583
(7) Burschka, J.; Pellet, N.; Moon S. J.; Humphry-Baker, R.; Gao, P; Nazeeruddin M. K.; Grätzel, M. *Nature* **2013**, *499*, 316
(8) Bi, D.; Tress, W.; Dar, M. I.; Gao, P.; Luo, J.; Renevier, C.; Schenk, K.; Abate, A.; Giordano, F.; Baena, J.-P. C.; Decoppet, J.-D.; Zakeeruddin, S. M.; Nazeeruddin, M. K.; Grätzel, M.; Hagfeldt, A. *Sci. Adv.* **2016**, *2*, e1501170
(9) Snaith, H.J.; Humphry-Baker, R.; Chen, P.; Cesar. I.; Zakeeruddin, S. M.; Grätzel, M. *Nanotechnology* **2008**, *19*, 424003
(10) Ding, I.-K.; Tétreault, N.; Brillet, J.; Hardin, B. E.; Smith, E. H.; Rosenthal, S. J.; Sauvage, F.; Grätzel, M.; McGehee, M. D. *Adv. Funct. Mater.* **2009**, *19*, 2431
(11) Mishra, A. Fischer, M. K. R.; Bäuerle, P. *Angew. Chem. Int. Ed.* **2009**, *48*, 2474
(12) Liang, M.; Chen, J. *Chem. Soc. Rev.* **2013**, *42*, 3453
(13) Zhang, X.; Grätzel, M.; Hua, J. *Front. Optoelectron.* **2016**, *9*, 3
(14) Lu, J.; Chang, Y.-C.; Cheng, H.-Y.; Wu, H.-P.; Cheng, Y.; Wang, M.; Diau, E. W.-G. *ChemSusChem* **2015**, *8*, 2529
(15) Nguyen, W. H.; Bailie, C. D.; Burschka, J.; Moehl, T.; Grätzel, M.; McGehee, M. D.; Sellinger, A. *Chem. Mater.* **2013**, *25*, 1519
(16) Burschka, J.; Dualeh, A.; Kessler, F.; Baranoff, E.; Cevey-Ha, N.-L.; Yi, C.; Nazeeruddin, M. K.; Grätzel, M. *J. Am. Chem. Soc.* **2011**, *133*, 18042
(17) Xu, B.; Huang, J.; Aagren, H.; Kloo, L.; Hagfeldt, A.; Sun, L. *ChemSusChem*, **2014**, *7*, 3252
(18) Xu, B.; Gabrielsson, E.; Safdari, M.; Cheng, M.; Hua, Y.; Tian, H.; Gardner, J. M.; Kloo, L.; Sun, L. *Adv. Energy Mater.* **2015**, *5*, 1402340
(19) Freitag, M.; Daniel, Q.; Pazoki, M.; Sveinbjörnsson, K.; Zhang, J.; Sun, L.; Hagfeldt, A.; Boschloo, G. *Energy Environ. Sci.* **2015**, *8*, 2634
(20) Wu, Y.; Zhu, W. *Chem. Soc. Rev.* **2013**, *42*, 2039
(21) Wu, Y.; Zhu, W.-H.; Zakeeruddin, S. M.; Grätzel, M. *ACS Appl. Mater. Interfaces* **2015**, *7*, 9307
(22) Mathew, S.; Yella, A.; Gao, P.; Humphry-Baker, R.; Curchod, B. F. E.; Ashari-Astani, N.; Tavernelli, I.; Rothlisberger, U.; Nazeeruddin M. K.; Grätzel M. *Nat. Chem.* **20014**, *6*, 242
(23) Zhang, X.; Mao, J.; Wang, D.; Li, X.; Yang, J.; Shen, Z.; Wu, W.; Li, J.; Ågren, H.; Hua, J. *ACS Appl. Mater. Interfaces* **2015**, *7*, 2760
(24) Lee, Y.; Jo, A.; Park, S. B. *Angew. Chem. Int. Ed.* **2015**, *54*, 15689
(25) Ronca, E.; Pastore, M.; Belpassi, L.; Tarantelli F.; Angelis, F. D. *Energy Environ. Sci.* **2013**, *6*, 183
(26) Yang, J.; Ganesan, P.; Teuscher, J.; Moehl, T.; Kim, Y. J.; Yi, C.; Comte, P.; Pei, K.; Holcombe, T. W.; Nazeeruddin, M. K.; Hua, J.; Zakeeruddin, S. M.; Tian, H.; Grätzel, M. *J. Am. Chem. Soc.* **2014**, *136*, 5722
(27) Haid S., Marszalek M., Mishra A., Wielopolski M, Teuscher J, Moser J. E., Humphry-Baker R, Zakeeruddin S. M., Grätzel M. , Bäuerle P, *Adv. Funct. Mater.* **2012**, 22, 1291

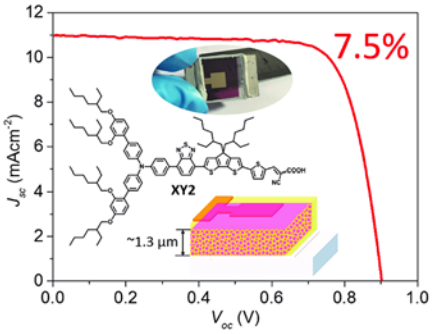
7.5%
XY2
~1.3 μm
J_{sc} (mAcm^{-2})
V_{oc} (V)
0
2
4
6
8
10
12
0.0
0.2
0.4
0.6
0.8
1.0